Shadow Art

Niloy J. Mitra
IIT Delhi / KAUST

Mark Pauly
ETH Zurich

Figure 1: *A 3D shadow art sculpture that simultaneously casts three distinct shadows. The side columns show the desired shadow image provided by the user (left), inconsistencies due to conflicting shadow constraints (middle), and optimized images (gray) that avoid shadow conflicts with the outline of the original for comparison (right).*

Abstract

"To them, I said, the truth would be literally nothing but the shadows of the images." - *Plato, The Republic*

Shadow art is a unique form of sculptural art where the 2D shadows cast by a 3D sculpture are essential for the artistic effect. We introduce computational tools for the creation of shadow art and propose a design process where the user can directly specify the desired shadows by providing a set of binary images and corresponding projection information. Since multiple shadow images often contradict each other, we present a geometric optimization that computes a 3D shadow volume whose shadows best approximate the provided input images. Our analysis shows that this optimization is essential for obtaining physically realizable 3D sculptures. The resulting shadow volume can then be modified with a set of interactive editing tools that automatically respect the often intricate shadow constraints. We demonstrate the potential of our system with a number of complex 3D shadow art sculptures that go beyond what is seen in contemporary art pieces.

1 Introduction

Shadows play an essential role in how we perceive the world and have for a long time captured the imagination of artists and stage performers. Our ability to recognize 3D objects from their 2D shadows and the fact that many different shapes can cast the same shadow are instrumental in the classical hand shadows and other forms of storytelling such as ancient Chinese shadow puppetry [Ewart 1998].

More recently, artists like Tim Noble and Sue Webster, or Shigeo Fukuda have created shadow art sculptures by assembling everyday objects into a seemingly random 3D ensemble (Figures 2 a-d). What makes these sculptures so compelling is that even though the 3D collage does not resemble any recognizable object, shadows cast by the sculptures create the illusion of a clearly recognizable scene. A variation of this theme is shown in Figures 2 e-g, where a 3D volume has been created that exhibits two or three distinct silhouettes when viewed from orthogonal view points.

In this paper we study the design of shadow art and present interactive tools for creating 3D shadow art sculptures. The user selects one or more binary images that define the desired shadow(s) and specifies the spatial arrangement of light sources (view points). From this input our system computes a conservative shadow hull that serves as a sculpting block for further editing. The main challenge in this computation arises from the fact that multiple shadows often contradict each other, i.e., no 3D shape exists that simultaneously satisfies all shadow constraints. We introduce a novel geometric optimization method that automatically finds a consistent shadow hull by deforming the input images. These deformations are derived such that the induced distortion is minimized. The computed shadow hull can then be edited using a set of interactive tools to create more interesting 3D sculptures. The system automatically ensures that all edits are consistent with the computed shadow images, thus lifting the burden on the user to manually control the often intricate shadow constraints arising from multiple shadow images within the same 3D sculpture. If desired, the edited shadow

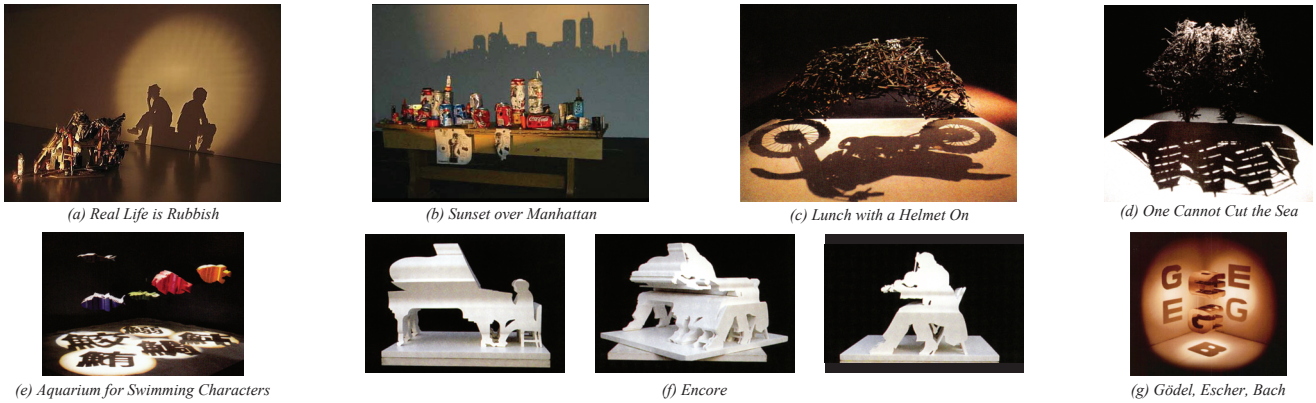

(a) Real Life is Rubbish *(b) Sunset over Manhattan* *(c) Lunch with a Helmet On* *(d) One Cannot Cut the Sea*

(e) Aquarium for Swimming Characters *(f) Encore* *(g) Gödel, Escher, Bach*

Figure 2: *Shadow sculptures by Tim Noble and Sue Webster (a, b ©Tim Noble & Sue Webster), Shigeo Fukuda (c, d, e, f ©Shigeo Fukuda), and Douglas Hofstadter (g ©Basic Books).*

volume can be filled automatically with a set of example shapes, mimicking the constructive approach of Figures 2 a-d.

Contributions. The main contributions of this paper are

- a formal description and analysis of shadow art, and the definition of suitable operators to compute a 3D shadow hull,
- a geometric optimization method that smoothly deforms the input images to satisfy the shadow constraints while minimizing the distortion induced by the deformation, and
- an interactive 3D editing toolbox that supports the exploration of the space of all possible sculptures that are consistent with a set of desired shadow images and allows the creation of constructive shadow art using an automated space-filling method.

To illustrate the artistic potential of our system, we have created a number of different 3D shadow sculptures. We argue that digital tools are essential in the design process to handle the complex shadow constraints, in particular when dealing with multiple shadows in a single sculpture.

Relation to Previous Work. Our work is mainly inspired by the 3D shadow art of modern artists such as Noble and Webster, or Fukuda (Figure 2). Numerous other artists have applied similar ideas in their work, typically using a manual, trial-and-error style approach to assemble 3D shadow sculptures. The digital design process we propose allows the creation of shadow sculptures that go beyond what we see in contemporary art pieces. For example, we can create (constructive) 3D shadow art sculptures that simultaneously satisfy three non-orthogonal shadows (Figure 1).

Shadows and visibility are central to many computer graphics applications and have been studied extensively both from a mathematical and perceptual point of view. Wanger and co-workers studied the effect of shadow quality on the perception of spatial relationships in computer generated imagery [Wanger et al. 1992; Wanger 1992]. An interface for interactive cinematic shadow design has been presented in [Pellacini et al. 2002], where the user indirectly modifies the positions of light sources and shadow blockers by specifying constraints on the desired shadows. Pocchiola and Vegter [1993] present a formal framework for studying visibility properties in a plane. Durand and colleagues [2002] analyzed the coherence and global nature of visibility for scenes composed of smooth convex objects. Even in this simplified setting, the resulting data structure has a complexity of $O(n^4)$ for n objects, indicating that a naïve global optimization of the visibility complex for our shadow art application is impractical.

Computing the shadow volume from a set of shadow images is similar to the construction of the visual hull used for 3D reconstruction from silhouettes. Originally introduced by Laurentini [1994], the visual hull is defined as the intersection volume of a set of generalized cones constructed from silhouette images and the corresponding camera locations. Reconstruction of closed continuous surfaces from multiple calibrated images using min-cuts with strict silhouette constraints has been studied by Sinha and Polleyfeys [2005]. The key difference to our setting is that in visual hull reconstruction, assuming accurate calibration, the silhouettes will always be consistent, since they result from projections of a real physical object. For arbitrary input images, such a 3D shape might not exist, which motivates our optimization approach that warps the input images to achieve consistency. This method has some similarities with the symmetrization technique introduced by Mitra and colleagues [2007] that warps a 3D shape to enhance its approximate symmetries. We do not explicitly account for symmetries, but could easily incorporate the symmetrizing constraints in our optimization.

Kutulakos and Seitz [1999] characterized the intrinsic ambiguities in reconstructing a 3D object using the visual hull. We exploit these ambiguities to enable interactive editing operations that modify the 3D shadow volume, but leave the desired 2D shadows intact. Our editing tools operate on a 3D voxel representation, similar to 3D sculpting tools, such as [Galyean and Hughes 1991]. Specific to our setting is the coupling of voxels induced by the shadow constraints that leads to a unique interactive design process. We support this process by automatically ensuring that all editing operations respect the shadow constraints. Gal and colleagues [2007] recently presented an interactive algorithm for designing a *3D collage*, a compound object formed by juxtaposing common geometric shapes. Our space-filling approach for creating constructive shadow art uses a similar strategy to increase the expressiveness of the 3D shape, but focuses mostly on the saliency of shadow boundaries. Our method also bears some resemblance to a recent shape morphing tool called *shadow metamorphosis* [Klimmek et al. 2007]. The general idea is to compute a Cartesian product of two shapes, e.g., a 4D product of two 2D silhouette images, and use projections of this object from different viewpoints to create a morph between the input shapes. This process resembles the construction shown in Figure 2 e-g, yet is fundamentally different due to the different dimensionality. The Cartesian product of n 2D shapes yields a $2n$ dimensional object, while we always operate with a 3D shadow volume. Sela and Elber [2007] propose non-realistic modeling based on B-splines surfaces. One of two 3D input models is deformed so that its silhouette matches the silhouette extracted from the second model for a specific view direction. In contrast, our approach constructs the shadow hull directly from the specified 2D shadow images.

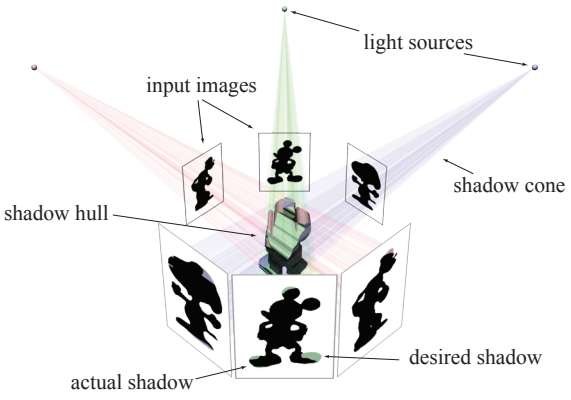

Figure 3: *Snoopy, Mickey, and Popeye meet in shadow art. A shadow source, specified by a projection and an input image, defines a generalized shadow cone. The intersection of these cones yields the shadow hull. Inconsistencies lead to deviations of the actual shadows from the desired shadow images.*

2 The Shadow Hull

The input to our system is a set $\mathcal{S} = \{S_1, \ldots, S_n\}$ of *shadow sources* $S_k = (I_k, P_k)$. The binary image I_k represents the desired shadow, while the projection P_k defines the spatial configuration of the shadow source (Figure 3). Currently, we support orthographic and perspective projections, i.e., shadows cast by directional light or point light sources. We comment on issues related to finite-extent area light sources in Section 5. Each shadow source S_k defines a generalized cone $C_k \subset \mathbb{R}^3$ that marks the maximum region of space compatible with I_k and P_k. Intersecting the shadow cones of the set $\mathcal{S}$ yields the 3D *shadow hull* $H(\mathcal{S}) = C_1 \cap \cdots \cap C_n$. The shadow hull can be seen as a sculpting block for a 3D shadow art piece. Any part of space outside the shadow hull cannot be part of the sculpture, since this would contradict at least one of the desired shadow images. However, typically a lot of material of the hull can be removed without violating the shadow constraints to create artistically pleasing results (see Section 4).

Consistency. Let I'_k be the actual shadow cast by the shadow hull H under projection P_k. We call a set of shadow sources *consistent*, if $I'_k = I_k$ for all k. As shown in Figure 3, shadow sources provided by the user need not be consistent. In fact, inconsistency is the rule rather than the exception for more than two shadow sources. Inconsistent shadow sources lead to a shadow hull that casts incomplete shadows, i.e., parts of the input shadow image will be missing, which can easily destroy the desired artistic effect. Finding a consistent set of shadow sources that closely resembles the user's input is one of the key challenges that we address in this paper. In Section 3 we introduce an optimization approach that aims at minimally altering the input images in order to achieve consistency.

Discretization. The input images I_k provided by the user are represented as binary pixel grids with $I_k(i,j) = 1$ for a shadow pixel and $I_k(i,j) = 0$ for a lit pixel. Analogously, we discretize the shadow hull H with a binary voxel grid, where $H(x,y,z) = 1$ denotes occupied voxels, while $H(x,y,z) = 0$ indicates empty space. We call pixels and voxels with $I_k(i,j) = 1$ or $H(x,y,z) = 1$ *active*, otherwise they are labeled as *empty*. To compute the shadow hull we simply map all voxel centers onto each of the different input images I_k using the projection P_k. The value of a specific cell is then evaluated using a binary AND operation on the corresponding image pixels. We favor the volumetric approach over a surface-based method, since subsequent editing of the shadow hull requires volumetric operations that are straightforward to define on a voxel grid. In addition, the regularity of the grid enables an efficient GPU implementation similar to [Ladikos et al. 2008]. Disadvantages of this approach are aliasing and grid alignment artifacts that we will comment on in Section 5.

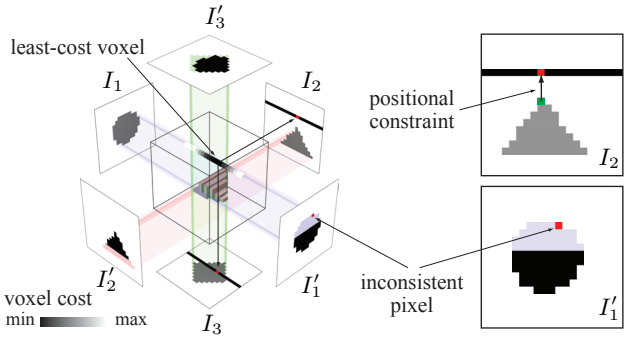

Figure 4: *An inconsistent pixel corresponds to a line of empty voxels shown with the respective cost value in gray-scale colors. The projection of the least-cost voxel provides the target location for a positional constraint of the deformation model. Pulling the green point towards the red pixel will deform image I_2 to resolve the inconsistency of the shadow I'_1.*

3 Optimization

The first step in the creation of shadow art sculptures is the specification of shadow sources. Our system allows the user to interactively modify the shadow projections that define the spatial configuration of the shadows, and to position, scale, and orient the input images. Since our GPU implementation achieves realtime performance, these modifications are supported by immediate visual feedback on the consistency of the resulting shadow images.

Yet consistency is difficult to achieve manually. Finding a consistent configuration for a given choice of input images might be impossible and our extensive experiments confirm that the existence of a consistent set of shadow sources is the exception for more than two shadow images. To overcome this limitation, we introduce an optimization approach that aims at finding a consistent set of images that is as close as possible to the provided input. The optimization exploits the fact that even small changes in one image can lead to drastic improvements in terms of shadow consistency of the other images. As illustrated in Figure 5, subtle image deformations can yield a consistent shadow hull without significantly altering the desired shadows. Yet manually specifying the deformations can be extremely cumbersome, since fixing one part of the model can easily invalidate other regions, due to the strong coupling of shadow constraints. Our solution resolves all inconsistencies simultaneously in a global optimization.

We employ the as-rigid-as possible shape manipulation method of [Igarashi et al. 2005] that computes a smooth deformation of an image using a 2D triangle mesh discretization of the image space. The optimization solves for vertex displacement vectors that are linearly interpolated to compute new positions for each image pixel. Given a set of positional constraints to drive the deformation we automatically derive these constraints by analyzing the shadow inconsistencies, i.e., the set of pixels that are active in the input images I_j, but empty in the corresponding shadow images I'_j.

Figure 4 provides a low-resolution illustration with three orthogonal input images I_1, I_2, I_3. Due to inconsistencies, the resulting shadow images I'_1, I'_2, I'_3 are incomplete. An inconsistent pixel in

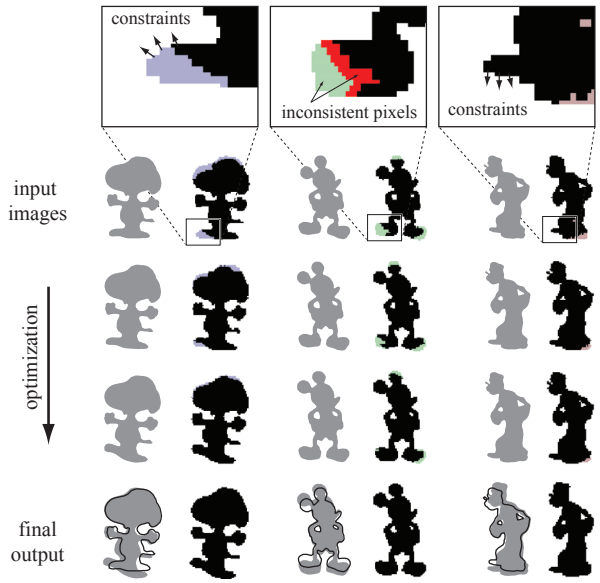

Figure 5: *The global optimization gradually deforms the images towards a consistent configuration. Colored pixels show inconsistencies of the shadow images. The zooms illustrate the positional constraints for parts of the snoopy and popeye images that have been computed to fix the inconsistency of Mickey's left foot marked in red. The remaining inconsistencies, marked in green, are considered in later iterations. The outlines in the bottom row indicate the deviation between the optimized images and the input images.*

I_1' corresponds to a line of empty voxels in the shadow hull. Setting any such voxel to active would fill the pixel in I_1'. However, these voxels project onto lines of pixels in I_2 and I_3 that lie completely outside the desired shadow silhouette in a least one of the images. Thus to realize such a pixel in I_1', we necessarily have to contradict at least one of the shadows of I_2 or I_3. We can assign a cost to such a shadow violation by measuring the minimal distance of all projected voxels to the boundary of the contradicted shadow; we take the sum of these distances if both I_2 and I_3 are violated. The least-cost voxel provides us with position constraints for the deformation. In the example of Figure 4 we select the projection of this voxel in image I_2 as the target location for the corresponding closest point on the shadow boundary. This will deform image I_2 towards a configuration that is likely to resolve the inconsistency at the selected pixel in I_1'.

Figure 5 shows different iteration stages of the optimization for the configuration shown in Figure 3. In each iteration, we select a thin layer of inconsistent pixels in each of the input images I_j, highlighted in red in the zoom of Mickey's foot. Using the construction of Figure 4, we derive corresponding positional constraints, indicated by arrows, for boundary pixels of the other input images and simultaneously apply the same procedure to all other images. Employing as-rigid-as possible shape manipulation [2005] to satisfy the desired positional constraints, we obtain a continuous displacement field for each image. Since small changes to one image can have drastic effects on the consistency of the others, we apply only a small fraction (0.25 in all examples) of the resulting displacements to the images. The positional constraints are then re-computed from the updated images, and the process repeated until a consistent configuration is achieved. Initially we use a high stiffness in the deformation model to automatically position the images relative to each other. Subsequently, stiffness is relaxed to allow non-rigid deformations. The process is stopped when the image deformation cost with respect to the input images exceeds a user-specified tolerance.

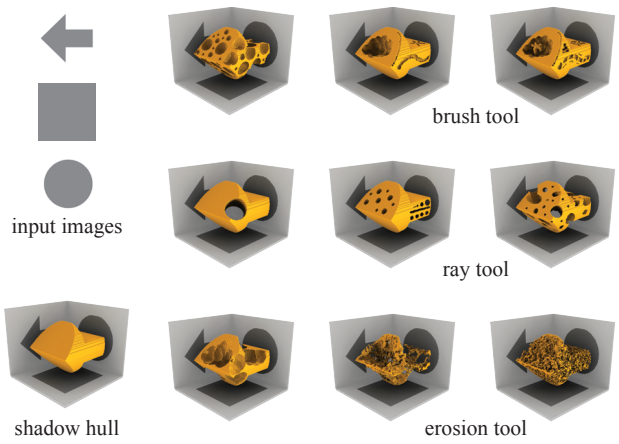

Figure 6: *The brush, ray, and erosion tools provide versatile editing functionality for modifying the 3D sculpture hull without altering the desired shadow images provided by the user.*

4 Editing

The result of the optimization yields a consistent shadow hull defining the maximal region of space that can possibly be occupied by the 3D sculpture. The shadow hull itself might already be the desired sculpture, as in the examples of Figures 2 e-g. We offer two additional methods for creating more interesting shadow art: a volumetric sculpting tool that allows interactive editing of the shadow volume and an example-based space filling method that mimics the constructive approach illustrated in Figures 2 a-d.

Volumetric Sculpting. In general, only a subset of the shadow hull is required to achieve the desired shadow images, leaving substantial freedom to create artistically pleasing 3D sculptures by removing material from the hull. The shadow constraints impose a strong non-local coupling between different parts of the shadow volume that dynamically changes as the sculpture is edited. This leads to a unique interactive design process, where local edits in some region can affect the flexibility of edits in other parts of the model. We introduce a number of editing tools to support the creation of compelling shadow art, a brush tool, a ray tool, and an erosion tool (see Figure 6). Similar to 2D painting applications, the brush tool allows the user to activate and de-activate shadow voxels using a variable-size 3D brush that selects all voxels within a spherical region around the focus point. In case the shadow constraints prohibit removing all selected voxels simultaneously, the user can choose between two options: either abort the removal operation altogether, or remove as many voxels of the brush selection as possible using a pre-defined traversal order. Since the penetration of light through the shadow sculpture is of particular importance for the resulting visual effect, the ray tool allows the user to select all voxels along a ray piercing the shadow hull. The selection is computed as the intersection of the shadow volume with a cylinder of varying radius. Voxels are only removed if the entire set can be deleted, so that light can pass through the volume in the direction of the ray. To simulate the effect of random erosion of the shape, we have implemented a snake that eats its way through the currently active voxel set, i.e., removes all voxels encountered in its traversal of the shadow volume, if compatible with the shadow constraints. A snake can be controlled by specifying its starting point and lifetime, as well as directional preferences. The erosion-like appearance in the resulting shadow sculpture can create artistically interesting effects that are tedius to achieve with direct editing.

Figure 7: *Three currency symbols combined in a sculpture built from Lego. Inconsistencies are marked in light gray in the bitmap images. The relative scaling is not preserved due to the elongation of Lego bricks in one direction. The black pedestal has been added for stability.*

Example-based Space Filling. If the user is satisfied with the edited shadow hull, the voxel grid is converted to a triangle mesh using contouring [Kazhdan et al. 2007]. A few steps of subdivision on the mesh yield a smooth surface that can, for example, be send to a 3D printer (see Figure 10). We also provide a tool for example-based design of the shadow sculptures inspired by the constructive approach that is popular with contemporary artists (Figures 2 a-d). Given a repository of 3D example shapes, we apply an iterative space filling method to fully automatically assemble the 3D sculpture. Initially, the entire shadow volume is marked as empty. The algorithm then selects a random shape from the repository and positions the shape randomly in an empty region of the shadow volume. This initial position is refined using a registration method that optimizes for a rigid transformation that brings the example shape into correspondence with the 3D shadow mesh [Rusinkiewicz and Levoy 2001]. We include additional inside-outside tests to guarantee that the example shape remains within the shadow volume. This approach is similar to recent work on expressive 3D modeling [Gal et al. 2007]. Our method differs mainly in that we focus primarily on 2D silhouette matching.

Figure 8 shows a 3D shadow sculpture that has been assembled fully automatically using our space filling approach. To our knowledge, artists have so far only considered this kind of constructive shadow art for single shadows, while our sculpture simultaneously satisfies three non-orthogonal shadows. The resulting shadow constraints are substantially more complex than for single shadows, making manual assembly particularly challenging.

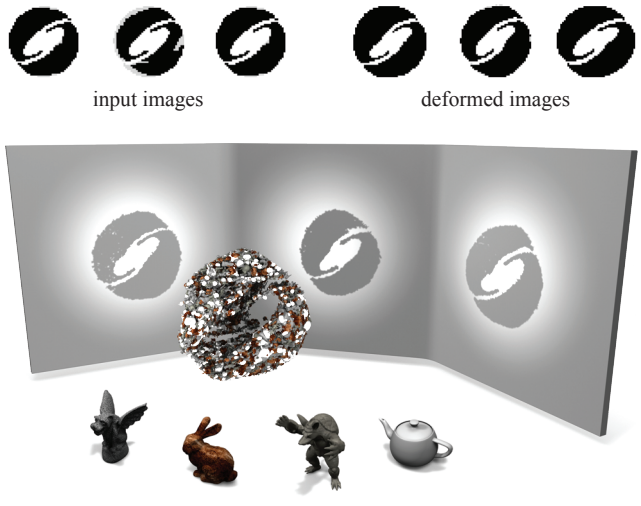

Figure 8: *Example-based shadow art. Well-known graphics models are used to create a constructive shadow art sculpture that casts three shadows at 45 degree angle depicting the Siggraph logo.*

5 Results

We have created a number of different 3D shadow art sculptures to illustrate the versatility of our approach. The visual effect of shadow art is often best appreciated in a dynamic setting where light source or view point are in motion (see accompanying video). Figure 1 shows a particularly challenging example with three concurrent shadows at 45 degree angle. The optimization significantly deforms the images, yet preserves the intricate geometric features of the animal silhouettes. The resulting shadow hull has been edited using the brush, ray, and erosion tools to create a complex geometric shape that looks substantially different than the input images from most viewpoints. Figure 7 depicts a sculpture with three orthogonal shadows built from Lego bricks. Here the direct construction without software support would be particularly tedious, since adding and removing individual voxels is complicated due to the specific construction constraints of Lego. An interesting question for future work is the automatic generation of suitable assembly instructions given a specific set of bricks. Figure 9 shows a shadow art tribute to Andy Warhol. This is the only example in the paper that does not require any image deformations to achieve consistency, since the projections are orthogonal and each image has a complete ring of active pixels at the boundary. Figure 10 shows a 3D printout of a shadow sculpture created from three cartoon silhouettes shown in Figure 3. Large shadows can be cast by the relatively small sculpture due to the strong perspective in this example. The model shown in Figure 13 combines three different shadow images of an articulated character positioned at 60 degree angles. Substantial image warping is required to achieve consistency, yet the overall appearance is well preserved, since the deformation model can easily be adapted to respect the shape semantics. Our system was also used in the production of *Silhouettes of Jazz*, an experimental animation depicting the history of traditional jazz music in a virtual walkthrough of a shadow art museum [Käser et al. 2009].

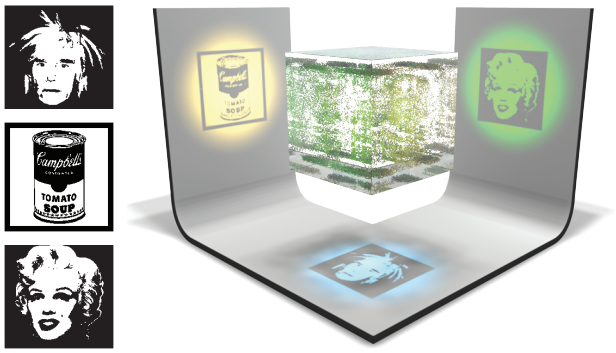

Figure 9: *A shadow art tribute to Andy Warhol. A seemingly random voxel soup embedded into a glass cube creates three distinct shadow images.*

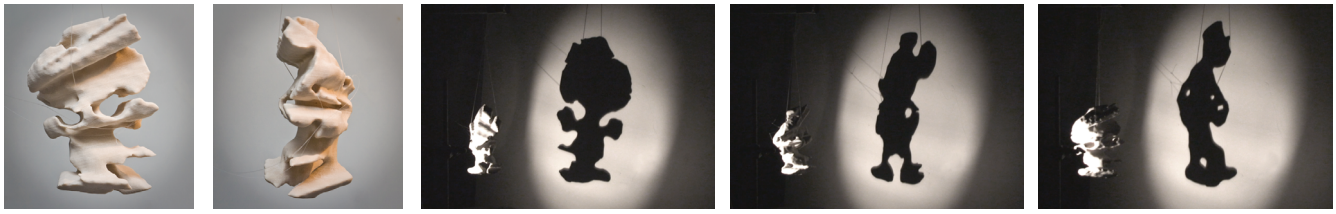

Figure 10: *A 3D printout of the example shown in Figure 5. Some features are lost due to restrictions of the 3D printer.*

Discussion and Limitations. As illustrated in the accompanying video and demo tool, our implementation achieves immediate visual feedback for the main stages of the pipeline, enabling an interactive, exploratory design process. All sculptures except the Lego example have an input image resolution of 250×250 and use a fixed set of parameters (set as default parameters in the demo). A key advantage of a digital approach to shadow art design is that the often complex, non-local shadow constraints are observed automatically, allowing the user to focus on artistic considerations. We found that the geometric optimization significantly increases the space of possible shadow image combinations, since substantial inconsistencies can be removed with subtle deformations that do not affect the shadow semantics significantly. However, not all combinations of images are suitable for creating shadow art, as illustrated in Figure 11. The input images are significantly warped, in the semantic sense, even when the as-rigid-as-possible deformation cost is low. The optimization, being a greedy one, can converge to a local minima when the initialization is poor.

All our computations are based on perspective or orthographic projections, hence we assume either ideal point light sources or parallel light. As a consequence, real physical light sources do not reproduce the desired shadows exactly, but lead to blurred shadow boundaries. We found that the benefits of this mathematical abstraction for the formulation of the algorithm and the resulting implementation outweigh the imprecisions of the resulting shadows. The softer appearance of shadows cast by area light sources can even be desirable for certain sculptures. Blurred shadow boundaries have an additional advantage: The discretization of the shadow hull using a voxel grid is prone to aliasing and grid alignment artifacts. Area light sources mitigate the resulting visual deficiencies due to the inherent low-pass filtering of shadow boundaries. Applying a few steps of subdivision to the mesh extracted from the voxel grid further reduces grid artifacts. For the example-based construction shown in Figure 8, grid artifacts are less critical, since the visual appearance mostly depends on the smoothness of the silhouettes of the example shapes.

The optimization does not consider structural aspects such as connectedness of the shadow hull that might be important for a physical realization of the sculpture. However, we can ensure that no additional components will be created during the editing stage. If the input images are composed of multiple components, the shadow hull necessarily consists of disconnected pieces. In such cases, the 3D sculpture can be embedded in a transparent medium, as illustrated in Figure 9 and 13. Alternatively, transparent threads or other thin supporting elements can be added to create a stable configuration as shown in Figure 1. Our automated space-filling approach does not prevent inter-object collisions, which would be important if the sculpture should be assembled from a given set of physical objects, rather than produced by e.g. a 3D printer, where self-intersections are less problematic. To resolve this issue a rigid-body collision library can be integrated into the system.

Minimum Sets. The editing tools described in Section 4 enable the user to explore the space of all 3D sculptures that are compatible with the given shadow constraints. An interesting theoretical question arises: What is the *smallest* voxel set that respects the shadow constraints? We can shed some light on this question by noting that the evaluation of the shadow constraints can be formulated as a special instance of a Boolean satisfiability problem [Clote and Kranakis 2002]. A simple analysis shows that for two orthogonal, orthographic shadow sources, the minimum set problem can be reduced to a bipartite graph matching problem, for which polynomial time algorithms exist. However, the same construction is not applicable for three shadows. We conjecture that finding the smallest consistent shadow sculpture in this case is *NP*-hard.

Other Applications. In this paper we focus on the creation of shadow art sculptures, yet other applications can also benefit from our optimization approach. For example, in 3D reconstruction based on visual hulls our method could reduce inconsistencies caused by inaccurate camera calibration or lens distortions. Figure 12 illustrates the application of our approach in sketch-based modeling [Olsen et al. 2008], where the user draws sketches of a shape from different viewpoints to quickly create a 3D model. Our optimization automatically corrects imprecisions in the drawings by warping the shape outlines toward a consistent configuration. Such a system offers a simple and intuitive user experience and could be combined with recent methods on shape design based on orthographic views [Thormählen and Seidel 2008].

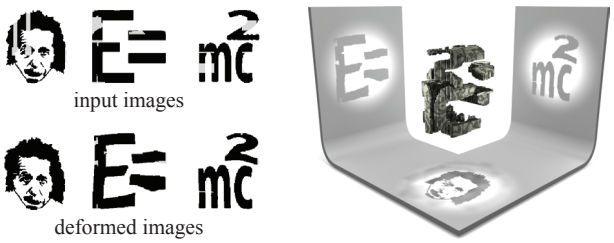

Figure 11: *For certain combinations of images, even strong deformations cannot resolve all inconsistencies.*

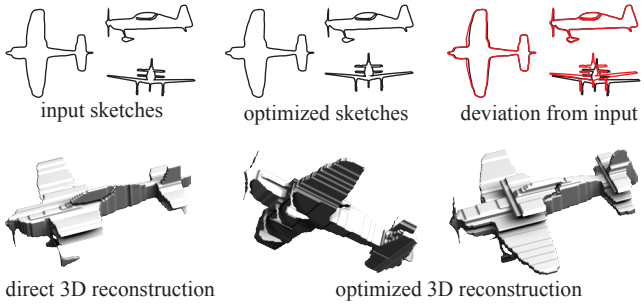

Figure 12: *Sketch-based model creation exploits our geometric optimization to warp the input drawings towards a consistent state.*

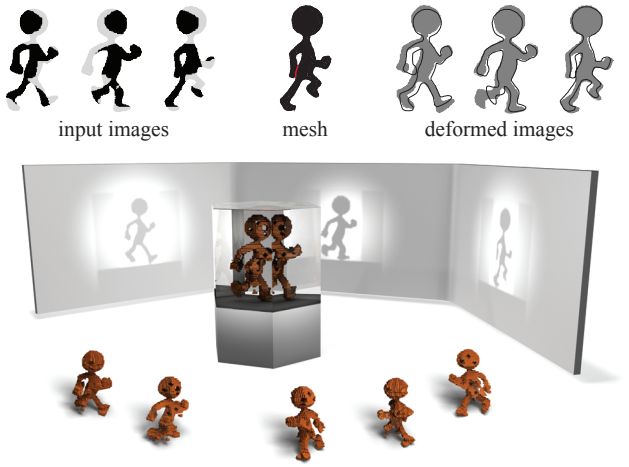

Figure 13: *A sculpture casts three shadow poses of an animated cartoon character at* 60 *degree angle. Substantial initial inconsistencies (shown as gray pixels) have been removed by the optimization. The red line indicates a topological surgery performed by the user on the deformation mesh to specify the shape semantics. Bottom row shows the sculpture from different viewpoints.*

6 Conclusion and Future Work

We have introduced a computational framework for interactive creation of 3D shadow art. The key enabling technique is a geometric optimization for constructing a consistent shadow hull from a set of inconsistent input images using shape-preserving deformations. We show that this optimization is essential for achieving the desired shadows. Our interactive editing tools allow the creation of complex 3D shadow sculptures, while automatically observing the intricate shadow constraints. We believe that our system can help to make this art form accessible to a broader audience and see several directions for future work, both from an artistic and a scientific point of view. Interesting questions arise in the analysis of the set of all subsets of the shadow hull that satisfy the shadow constraints. Connections to Boolean satisfiability, minimum set cover, and graph coloring problems, are immediate and can potentially lead to new theoretical insights. So far we consider only opaque materials and hence black-and-white shadow images. Semi-transparent materials offer the potential for gray-scale shadows that would pose challenging questions both for optimization and interaction. Our current system is designed for static shadow sculptures. Interesting artistic effects can also be achieved with dynamic shadow art, where multiple moving parts can create animated shadows.

Acknowledgements. This work is supported by a Microsoft Outstanding Young Faculty Fellowship and the Swiss National Science Foundation. We thank Karan Singh for many helpful suggestions, Michael Kazhdan for providing code for isosurface extraction, and Subhashis Banerjee, Naveen Garg, Leonidas Guibas and Helmut Pottmann for sharing their thoughts on the project. We want to specially thank Dominik Käser, Martin-Sebastian Senn, and Mario Deuss for their dedication, hard work, and enthusiasm while helping with coding, illustrations, and preparing the final video.

References

CLOTE, P., AND KRANAKIS, E. 2002. *Boolean Functions and Computation Models*. Springer.

DURAND, F., DRETTAKIS, G., AND PUECH, C. 2002. The 3D visibility complex. *ACM Trans. Graph. 21*, 2, 176–206.

EWART, F. G. 1998. *Let The Shadows Speak*. Trentham Books.

GAL, R., SORKINE, O., POPA, T., SHEFFER, A., AND COHEN-OR, D. 2007. 3D collage: Expressive non-realistic modeling. In *Proc. of NPAR*, 7–14.

GALYEAN, T. A., AND HUGHES, J. F. 1991. Sculpting: an interactive volumetric modeling technique. In *Proc. of SIGGRAPH*, 267–274.

IGARASHI, T., MOSCOVICH, T., AND HUGHES, J. F. 2005. As-rigid-as-possible shape manipulation. *ACM SIGGRAPH Trans. Graph. 24*, 3.

KÄSER, D., SENN, M.-S., DEUSS, M., PAULY, M., AND MITRA, N. J., 2009. Silhouettes of jazz. SIGGRAPH Computer Animation Festival. http://www.silhouettesofjazz.com.

KAZHDAN, M., KLEIN, A., DALAL, K., AND HOPPE, H. 2007. Unconstrained isosurface extraction on arbitrary octrees. In *Proc. of Symp. of Geometry Processing*, 125–133.

KLIMMEK, B., PRAUTZSCH, H., AND VAHRENKAMP, N. 2007. Shadow metamorphosis. *Computing 79*, 2, 325–335.

KUTULAKOS, K. N., AND SEITZ, S. M. 1999. A theory of shape by space carving. *Int. Journal of Computer Vision 38*, 307–314.

LADIKOS, A., BENHIMANE, S., AND NAVAB, N. 2008. Efficient visual hull computation for real-time 3D reconstruction using CUDA. In *Proc. of CVPR Workshops*.

LAURENTINI, A. 1994. The visual hull concept for silhouette-based image understanding. *Trans. on PAMI 16*, 2, 150–162.

MITRA, N. J., GUIBAS, L. J., AND PAULY, M. 2007. Symmetrization. *ACM SIGGRAPH Trans. Graph. 26*, 3, #63.

OLSEN, L., SAMAVATI, F., SOUSA, M., AND JORGE, J. 2008. Sketch-based modeling: A survey. *Computers and Graphics*.

PELLACINI, F., TOLE, P., AND GREENBERG, D. P. 2002. A user interface for interactive cinematic shadow design. *ACM SIGGRAPH Trans. Graph. 21*, 3, 563–566.

POCCHIOLA, M., AND VEGTER, G. 1993. The visibility complex. In *Proc. of the ACM Symposium on Computational Geometry*, 328–337.

RUSINKIEWICZ, S., AND LEVOY, M. 2001. Efficient variants of the ICP algorithm. *3DIM*, 145–152.

SELA, G., AND ELBER, G. 2007. Generation of view dependent models using free form deformation. *The Visual Computer 23*, 3, 219–229.

SINHA, S. N., AND POLLEFEYS, M. 2005. Multi-view reconstruction using photo-consistency and exact silhouette constraints: A maximum-flow formulation. In *IEEE ICCV*, 349–356.

THORMÄHLEN, T., AND SEIDEL, H.-P. 2008. 3D-modeling by ortho-image generation from image sequences. *ACM SIGGRAPH Trans. Graph. 27*, 3, 1–5.

WANGER, L. C., FERWERDA, J. A., AND GREENBERG, D. P. 1992. Perceiving spatial relationships in computer-generated images. *IEEE Comput. Graph. Appl. 12*, 3, 44–51, 54–58.

WANGER, L. 1992. The effect of shadow quality on the perception of spatial relationships in computer generated imagery. In *Proc. of the Symp. on Interactive 3D graphics*, 39–42.